Simple analytical expression for crosstalk estimation in homogeneous trench-assisted multi-core fibers

Ye, Feihong; Tu, Jiajing; Saitoh, Kunimasa; Morioka, Toshio

Published in:
Optics Express

Link to article, DOI:
10.1364/OE.22.023007

Publication date:
2014

Document Version
Publisher's PDF, also known as Version of record

Simple analytical expression for crosstalk estimation in homogeneous trench-assisted multi-core fibers

Feihong Ye,[1,*] Jiajing Tu,[2] Kunimasa Saitoh,[2] and Toshio Morioka[1]

[1]*DTU Fotonik, Department of Photonics Engineering, Technical University of Denmark, DK-2800 Kgs. Lyngby, Denmark*

[2]*Graduate School of Information Science and Technology, Hokkaido University, Sapporo, 060-0814, Japan*

[*]*feye@fotonik.dtu.dk*

Abstract: An analytical expression for the mode coupling coefficient in homogeneous trench-assisted multi-core fibers is derived, which has a simple relationship with the one in normal step-index structures. The amount of inter-core crosstalk reduction (in dB) with trench-assisted structures compared to the one with normal step-index structures can then be written by a simple expression. Comparison with numerical simulations confirms that the obtained analytical expression has very good accuracy for crosstalk estimation. The crosstalk properties in trench-assisted multi-core fibers, such as crosstalk dependence on core pitch and wavelength-dependent crosstalk, can be obtained by this simple analytical expression.

OCIS codes: (060.2270) Fiber characterization; (060.2330) Fiber optics communications.

References and links

1. T. Morioka, "New generation optical infrastructure technologies: 'EXAT initiative' towards 2020 and beyond," in Proc. OECC (2009), paper FT4.
2. S. Matsuo, M. Ikeda, and K. Himeno, "Bend-insensitive and low-splice-loss optical fiber for indoor wiring in FTTH," in Proc. OFC (2004), paper ThI3.
3. K. Takenaga, Y. Arakawa, S. Tanigawa, N. Guan, S. Matsuo, K. Saitoh, and M. Koshiba, "Reduction of crosstalk by trench-assisted multi-core fiber," in Proc. OFC (2011), paper OWJ4.
4. J. Sakaguchi, B. J. Puttnam, W. Klaus, Y. Awaji, N. Wada, A. Kanno, T. Kawanishi, K. Imamura, H. Inaba, K. Mukasa, R. Sugizaki, T. Kobayashi, and M. Watanabe "305 Tb/s space division multiplexed transmission using homogeneous 19-core fiber," J. Lightwave Technol. **31**, 554–562 (2013).
5. H. Takara, A. Sano, T. Kobayashi, H. Kubota, H. Kawakami, A. Matsuura, Y. Miyamoto, Y. Abe, H. Ono, K. Shikama, Y. Goto, K. Tsujikawa, Y. Sasaki, I. Ishida, K. Takenaga, S. Matsuo, K. Saitoh, M. Koshiba, and T. Morioka "1.01-Pb/s (12 SDM/222 WDM/456 Gb/s) crosstalk-managed transmission with 91.4-b/s/Hz aggregate spectral efficiency," in Proc. ECOC (2012), paper Th.3.C.1.
6. K. Saitoh, T. Matsui, T. Sakamoto, M. Koshiba, and S. Tomita, "Multi-core hole-assisted fibers for high core density space division multiplexing," in Proc. OECC (2010), paper 7C2-1.
7. B. Yao, K. Ohsono, N. Shiina, K. Fukuzato, A. Hongo, E. H. Sekiya, and K. Saito, "Reduction of crosstalk by hole-walled multi-core fibers," in Proc. OFC (2012), paper OM2D.5.
8. K. Takenaga, Y. Arakawa, Y. Sasaki, S. Tanigawa, S. Matsuo, K. Saitoh, and M. Koshiba, "A large effective area multi-core fibre with an optimised cladding thickness," in Proc. ECOC (2011), paper Mo.1.LeCervin.2.
9. S. Matsuo, K. Takenaga, Y. Arakawa, Y. Sasaki, S. Taniagwa, K. Saitoh, and M. Koshiba, "Large-effective-area ten-core fiber with cladding diameter of about 200μm," Opt. Lett. **36**, 4626–4628 (2011).
10. S. Matsuo, Y. Sasaki, T. Akamatsu, I. Ishida, K. Takenaga, K. Okuyama, K. Saitoh, and M. Kosihba, "12-core fiber with one ring structure for extremely large capacity transmission," Opt. Express **20**, 28398–28408 (2012).

#217749 - $15.00 USD Received 24 Jul 2014; revised 28 Aug 2014; accepted 8 Sep 2014; published 15 Sep 2014

11. F. Ye, J. Tu, K. Saitoh, and T. Morioka, "Theoretical investigation of inter-core crosstalk properties in homogeneous trench-assisted multi-core fibers," in IEEE Photonics Society Summer Topicals Meeting Series (2014), paper TuE4.2.
12. F. Ye, J. Tu, K. Saitoh, H. Takara, and T. Morioka, "Wavelength-dependent crosstalk in trench-assisted multi-core fibers," in Proc. OECC/ACOFT (2014), paper TU5C1.
13. K. Okamoto, *Fundamentals of Optical Waveguides*, 2nd ed. (Academic Press, 2006).
14. J. Tu, K. Saitoh, M. Koshiba, K. Takenaga, and S. Matsuo, "Design and analysis of large-effective-area heterogeneous trench-assisted multi-core fiber," Opt. Express **20**, 15157–15170 (2012).
15. T. Hayashi, T. Taru, O. Shimakawa, T. Sasaki, and E. Sasaoka, "Low-loss and large-Aeff multi-core fiber for SNR enhancement," in Proc. ECOC (2012), paper Mo.1.F.3.
16. A. Snyder and J. D. Love, *Optical Waveguide Theory*, 1st ed. (Springer, 1983).
17. K. Imamura, K. Mukasa, and T. Yagi, "Effective space division multiplexing by multi-core fibers," in Proc. ECOC (2010), paper P1.09.

1. Introduction

Space-division multiplexing (SDM) is a promising candidate to overcome the capacity limit of single-mode fibers (SMFs) so as to sustain the rapid Internet traffic growth [1]. SDM based on uncoupled multi-core fibers (MCFs) is a simple and robust option, which requires no complex multiple-input multiple-output signal processing at the receiver side.

The main issue with high capacity MCF transmission is how we can increase the number of cores (thus, total capacity) while keeping the inter-core crosstalk (XT) low to allow higher multi-level modulation formats and longer transmission distance since more dense cores (smaller core pitch) normally increase the modes coupling among cores. The trench-assisted structure, based on its strong mode confinement capability, was originally proposed to reduce the fiber bending loss for FTTH applications [2]. The structure was then proposed to be applied to each core in MCFs for XT reduction [3], and capacity records experiments of both 305 Tb/s [4] and 1.01 Pb/s [5] transmission adopted trench-assisted structures, taking advantage of its low XT. Other XT reduction techniques such as hole-assisted [6], hole-walled [7] structures were also proposed. The relationships between the XT and the fiber parameters, such as relative refractive index difference between trench and cladding, trench width in trench-assisted multi-core fibers (TA-MCFs), however, have not been formulated analytically, and thus, the estimations of the XT in TA-MCFs in all the reported works so far [3, 8–10] have been done by numerical simulations and experimental measurements. In order to design MCFs with ultra-low XT for long distance and high capacity MCF transmission, however, it is important to understand the effects of these various fiber parameters on the XT reduction in TA-MCFs based on an analytical expression.

In this paper, we derive an analytical expression for the mode coupling coefficient in TA-MCFs, where the amount of XT reduction (in dB) by trench-assisted structure relative to normal step-index structure is given by a simple expression. The XT calculated by the derived analytical expression agree very well with those simulated by finite element method. In addition to the possibility of fast and accurate XT estimations in trench-assisted structure, the analytical expression can also be used to analyze the XT properties, such as XT dependence on core pitch [11] and wavelength-dependent XT [12].

This paper is divided into 5 sections. In section 2, the mode coupling coefficient in trench-assisted structure is formulated by relating to the one in normal step-index structure. Some appropriate approximation techniques are used in the derivation so that it can be simplified into an analytical expression. In section 3, the derived mode coupling coefficient is related to the XT and the amount of XT reduction (in dB) in TA-MCFs relative to normal step-index MCFs is formulated. In section 4, the results and discussions are presented. Firstly, XT estimations based on analytical expression and numerical simulations are compared, and it has been confirmed that the results obtained by our simplified analytical expression are in good agreement with

#217749 - $15.00 USD Received 24 Jul 2014; revised 28 Aug 2014; accepted 8 Sep 2014; published 15 Sep 2014

those based on finite element method. Secondly, further reduction of XT in trench-assisted structure is described. Section 5 concludes the work.

2. Mode coupling coefficient formulations

The refractive index profiles for normal step-index and trench-assisted structures are shown in Figs. 1(a) and 1(b), respectively. The refractive indices for the core, cladding and trench are n_1, n_0 and n_2, respectively, where the refractive indices in the 1st and 2nd claddings in trench-assisted structure are assumed to be the same. The relative refractive index differences between core and cladding, trench and cladding are Δ_1 and Δ_2, respectively. The core radius, the distance from the outer edge of the 1st cladding to the core center, the distance from the outer edge of trench to the core center and trench width are a_1, a_2, a_3 and w_{tr}, respectively. To have easy comparison, the core radius a_1, the relative refractive index difference between core and cladding Δ_1 in both structures are assumed to be the same.

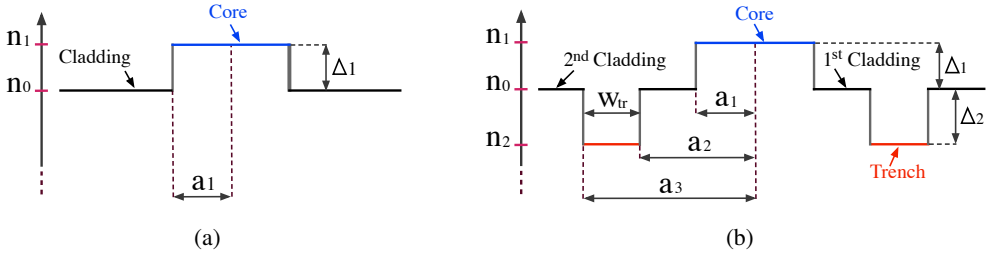

Fig. 1. Refractive index profiles and cross-sectional dimensions for (a) a normal step-index structure and (b) a trench-assisted structure.

2.1. *Normal step-index MCFs*

The mode coupling coefficient of directional coupler [13] is written as

$$\kappa'_{pq} = \frac{\omega\varepsilon_0 \int_{-\infty}^{\infty}\int_{-\infty}^{\infty}(N^2 - N_q^2)\mathbf{E}_p^* \cdot \mathbf{E}_q \, dxdy}{\int_{-\infty}^{\infty}\int_{-\infty}^{\infty}\mathbf{u}_z \cdot (\mathbf{E}_p^* \times \mathbf{H}_p + \mathbf{E}_p \times \mathbf{H}_p^*)\, dxdy}, \tag{1}$$

where ω is an angular frequency of the electromagnetic fields, ε_0 is the permittivity of vacuum, $N^2(x,y)$ denotes the refractive index distribution in the entire coupled region, N_q^2 represents the refractive index distribution of waveguide q (which includes core q and cladding in MCFs), * denotes the complex conjugate and $\mathbf{u}_z$ is a unit vector.

The mode coupling coefficient between two neighboring cores with step-index profiles in a directional coupler can then be simplified to [13]

$$\kappa'_{pq} = \frac{\sqrt{\Delta_1}}{a_1}\frac{U_1^2}{V_1^3 K_1^2(W_1)}\sqrt{\frac{\pi a_1}{W_1\Lambda}}\exp\Big(-\frac{W_1}{a_1}\Lambda\Big), \tag{2}$$

where $U_1^2 = a_1^2(k^2 n_1^2 - \beta^2)$ and $W_1^2 = a_1^2(\beta^2 - k^2 n_0^2)$, in which β is the propagation constant. $V_1 = k a_1 n_1 (2\Delta_1)^{1/2}$ is the V number which determines the modes propagating in a fiber, where $k = 2\pi/\lambda$ is the wave number and λ is the wavelength of light in vacuum. $K_1(W_1)$ is the modified Bessel function of the 2nd kind with 1st order and Λ is the core pitch (or core-to-core distance).

In order to compare with the mode coupling coefficient in a trench-assisted structure, formulated in Eq. (33) in [14], the mode coupling coefficient in normal step-index structure should

#217749 - $15.00 USD Received 24 Jul 2014; revised 28 Aug 2014; accepted 8 Sep 2014; published 15 Sep 2014

also be expressed in a similar form. With Eq. (4.118a) in [13] and $z = r/a_1$, the integral part of Eq. (4.117) in [13] can be written as

$$\int_0^{2\pi}\int_0^{a_1} J_0\Big(\frac{U_1}{a_1}r\Big)\exp\Big(\frac{W_1}{a_1}r\cos\theta\Big)r\,dr\,d\theta = 2\pi\int_0^{a_1} J_0\Big(\frac{U_1}{a_1}r\Big)I_0\Big(\frac{W_1}{a_1}r\Big)r\,dr, \tag{3}$$

where $J_0(U_1 r/a_1)$ is the Bessel function of the 1st kind with zero order and $I_0(W_1 r/a_1)$ is the modified Bessel function of the 1st kind with zero order, in which r is the radial distance from the center of the fiber core.

Finally, the mode coupling coefficient of directional coupler with normal step-index profiles can also be expressed as

$$\kappa_{pq}^{'} = k(n_1^2 - n_0^2)\frac{W_1^2}{n_1 a_1^2 V_1^2 J_1^2(U_1)}\frac{J_0(U_1)}{K_0(W_1)}\sqrt{\frac{\pi a_1}{2W_1\Lambda}}\exp\Big(-\frac{W_1}{a_1}\Lambda\Big)\int_0^{a_1} J_0\Big(\frac{U_1}{a_1}r\Big)I_0\Big(\frac{W_1}{a_1}r\Big)r\,dr, \tag{4}$$

where $J_1(U_1)$ is the Bessel function of the 1st kind with 1st order and $K_0(W_1)$ is the modified Bessel function of the 2nd kind with zero order.

2.2. *Trench-assisted MCFs*

As the sizes of the 1st cladding and the trench in trench-assisted structure are not infinitely large, the solutions in these two regions also contain the modified Bessel functions of the 1st kind $I_0(W_1 r/a_1)$, which makes the derivation of the mode coupling coefficient in TA-MCFs difficult. If $I_0(W_1 r/a_1)$ in the 1st cladding and the trench are ignored, the mode coupling coefficient between two adjacent cores in heterogeneous TA-MCFs can be written as Eq. (33) in [14], which can then be further simplified to the following for homogeneous case

$$\begin{aligned}\kappa_{pq}^{''} = {} & \frac{k(n_1^2 - n_0^2)W_1 U_1 L_q}{n_1 a_1^2 V_1^2 J_1^2(U_1)}\sqrt{\frac{\pi a_1}{2W_1\Lambda}}\exp\Big(-\frac{W_1}{a_1}\Lambda\Big)\int_0^{a_1} J_0\Big(\frac{U_1}{a_1}r\Big) \\ & \times I_0\Big[\Big(\frac{W_1}{a_1} + \frac{P_1 - P_2 + Y_1 - Y_2}{\Lambda - r}\Big)r\Big]\exp\Big(-\frac{P_1 - P_2 + Y_1 - Y_2}{\Lambda - r}\Lambda\Big)r\,dr,\end{aligned} \tag{5}$$

where L_q, P_1, P_2, Y_1, Y_2 and $P_1 - P_2 + Y_1 - Y_2$ can be expressed as

$$\begin{cases} L_q = \dfrac{J_1(U_1)K_1(W_1 a_2/a_1)K_1(W_2 a_3/a_1)}{K_1(W_1)K_1(W_2 a_2/a_1)K_1(W_1 a_3/a_1)}, \\ P_1 = W_1\dfrac{\Lambda - a_3}{a_1}, \quad P_2 = W_2\dfrac{\Lambda - a_3}{a_1}, \\ Y_1 = W_2\dfrac{\Lambda - a_2}{a_1}, \quad Y_2 = W_1\dfrac{\Lambda - a_2}{a_1}, \\ P_1 - P_2 + Y_1 - Y_2 = (W_2 - W_1)\dfrac{a_3 - a_2}{a_1} = (W_2 - W_1)\dfrac{w_{tr}}{a_1}, \end{cases} \tag{6}$$

respectively, where $W_2 = (V_2^2 + W_1^2)^{1/2}$, in which $V_2 = k a_1 (n_0^2 - n_2^2)^{1/2}$.

Comparing Eq. (4) with Eq. (5), we have

$$\frac{\kappa_{pq}^{''}}{\kappa_{pq}^{'}} = \frac{U_1 L_q\int_0^{a_1} J_0\Big(\frac{U_1}{a_1}r\Big)I_0\Big[\Big(\frac{W_1}{a_1} + \frac{P_1 - P_2 + Y_1 - Y_2}{\Lambda - r}\Big)r\Big]\exp\Big(-\frac{P_1 - P_2 + Y_1 - Y_2}{\Lambda - r}\Lambda\Big)r\,dr}{W_1\dfrac{J_0(U_1)}{K_0(W_1)}\displaystyle\int_0^{a_1} J_0\Big(\frac{U_1}{a_1}r\Big)I_0\Big(\frac{W_1}{a_1}r\Big)r\,dr}. \tag{7}$$

#217749 - $15.00 USD Received 24 Jul 2014; revised 28 Aug 2014; accepted 8 Sep 2014; published 15 Sep 2014

For large arguments of ax and $(a+b)x$, the modified Bessel function of the 1st kind can be approximated as

$$I_0(ax) \approx \frac{1}{\sqrt{2\pi ax}}\exp(ax), \qquad I_0[(a+b)x] \approx \frac{1}{\sqrt{2\pi(a+b)x}}\exp[(a+b)x], \tag{8}$$

respectively, where $a > b > 0$.

If b is relatively small compared to a, $I_0[(a+b)x]$ can be related to $I_0(ax)$ by the following expression with good accuracy using the above relationship

$$I_0[(a+b)x] \approx \sqrt{\frac{a}{a+b}}\, I_0(ax)\exp(bx). \tag{9}$$

It should be noted that the approximation in Eq. (8) is valid only for large ax and $(a+b)x$, while Eq. (9) is also valid even when $(a+b)x$ is small. Typical value of Λ (i.e. 30 μm) can be more than 5 times larger than trench width (i.e. 4.5 μm), thus $(P_1 - P_2 + Y_1 - Y_2)/(\Lambda - r) = (W_2 - W_1)w_{\mathrm{tr}}/[a_1(\Lambda - r)] > 0$ is much smaller than W_1/a_1. Following Eq. (9), we have

$$I_0\left[\left(\frac{W_1}{a_1} + \frac{P_1 - P_2 + Y_1 - Y_2}{\Lambda - r}\right)r\right] \approx \sqrt{\Gamma}\, I_0\left(\frac{W_1}{a_1}r\right)\exp\left(\frac{P_1 - P_2 + Y_1 - Y_2}{\Lambda - r}r\right), \tag{10}$$

where Γ can be simplified to

$$\Gamma = \frac{W_1/a_1}{W_1/a_1 + (P_1 - P_2 + Y_1 - Y_2)/\Lambda} = \frac{W_1}{W_1 + (W_2 - W_1)w_{\mathrm{tr}}/\Lambda}, \tag{11}$$

in which r has been dropped since $(P_1 - P_2 + Y_1 - Y_2)/(\Lambda - r)$ is much smaller than W_1/a_1 and r is much smaller than Λ.

Substituting Eq. (10) into Eq. (7), the ratio between the mode coupling coefficients for the two structures becomes

$$\begin{aligned}
\frac{\kappa''_{\mathrm{pq}}}{\kappa'_{\mathrm{pq}}} &= \frac{U_1 L_{\mathrm{q}} \int_0^{a_1} J_0\left(\frac{U_1}{a_1}r\right)\sqrt{\Gamma}\, I_0\left(\frac{W_1}{a_1}r\right)\exp\left(\frac{P_1 - P_2 + Y_1 - Y_2}{\Lambda - r}r\right)\exp\left(-\frac{P_1 - P_2 + Y_1 - Y_2}{\Lambda - r}\Lambda\right)r\,dr}{W_1 \frac{J_0(U_1)}{K_0(W_1)} \int_0^{a_1} J_0\left(\frac{U_1}{a_1}r\right) I_0\left(\frac{W_1}{a_1}r\right) r\,dr} \\
&= \frac{\sqrt{\Gamma}U_1 L_{\mathrm{q}} \int_0^{a_1} J_0\left(\frac{U_1}{a_1}r\right) I_0\left(\frac{W_1}{a_1}r\right)\exp\left[-(P_1 - P_2 + Y_1 - Y_2)\frac{\Lambda - r}{\Lambda - r}\right]r\,dr}{W_1 \frac{J_0(U_1)}{K_0(W_1)} \int_0^{a_1} J_0\left(\frac{U_1}{a_1}r\right) I_0\left(\frac{W_1}{a_1}r\right) r\,dr} \\
&= \frac{\sqrt{\Gamma}U_1 L_{\mathrm{q}} \exp[-(P_1 - P_2 + Y_1 - Y_2)]}{W_1 \frac{J_0(U_1)}{K_0(W_1)}}.
\end{aligned} \tag{12}$$

Assuming $n = 1$ in the dispersion equation Eq. (3.71) for step-index fiber in [13], thus

$$\frac{J_0(U_1)}{U_1 J_1(U_1)} = \frac{K_0(W_1)}{W_1 K_1(W_1)}. \tag{13}$$

Substituting Eq. (13) into Eq. (12), we get

$$\frac{\kappa''_{\mathrm{pq}}}{\kappa'_{\mathrm{pq}}} = \frac{\sqrt{\Gamma}L_q \exp[-(P_1 - P_2 + Y_1 - Y_2)]}{\frac{J_1(U_1)}{K_1(W_1)}}. \tag{14}$$

#217749 - $15.00 USD Received 24 Jul 2014; revised 28 Aug 2014; accepted 8 Sep 2014; published 15 Sep 2014

For $x \geq 2$, the modified Bessel function of the 2nd kind can be approximated as

$$K_1(x) \approx K_0(x) \approx \sqrt{\frac{\pi}{2x}} \exp(-x). \tag{15}$$

Thus, L_q in Eq. (6) can be simplified to

$$L_q = \frac{J_1(U_1)}{K_1(W_1)} \exp\Big[-(W_2 - W_1)\frac{w_{tr}}{a_1}\Big]. \tag{16}$$

Finally, the ratio between the mode coupling coefficients for the two structures becomes

$$\frac{\kappa''_{pq}}{\kappa'_{pq}} = \sqrt{\Gamma}\exp[-(P_1 - P_2 + Y_1 - Y_2)]\exp\Big[-(W_2 - W_1)\frac{w_{tr}}{a_1}\Big] = \sqrt{\Gamma}\exp\Big[-2(W_2 - W_1)\frac{w_{tr}}{a_1}\Big]. \tag{17}$$

Replacing κ'_{pq} with Eq. (2), the mode coupling coefficient between two neighboring cores with trench-assisted structures in a directional coupler can then be expressed as

$$\kappa''_{pq} = \frac{\sqrt{\Gamma}\sqrt{\Delta_1}}{a_1} \frac{U_1^2}{V_1^3 K_1^2(W_1)} \sqrt{\frac{\pi a_1}{W_1 \Lambda}} \exp\Big[-\frac{W_1\Lambda + 2(W_2 - W_1)w_{tr}}{a_1}\Big]. \tag{18}$$

3. Relating mode coupling coefficients to inter-core crosstalk

The statistical mean of the XT (mean XT, XT_μ) between two adjacent cores of a homogeneous MCF [15] can be expressed as

$$XT_\mu \approx \frac{2\kappa_{pq}^2 R_b}{\beta\Lambda} L, \tag{19}$$

where R_b is the bending radius and L is the fiber length.

Substituting Eqs. (2) and (18) into the above expression, the analytical expressions for XT in normal step-index MCFs and TA-MCFs can be formulated, respectively.

For the estimations of XT reduction, the only difference between trench-assisted and normal step-index structures comes from the mode coupling coefficient, and the ratio of XT for the two different structures becomes

$$\frac{XT''_\mu}{XT'_\mu} = \left(\frac{\kappa''_{pq}}{\kappa'_{pq}}\right)^2 = \Gamma \exp\Big[-4(W_2 - W_1)\frac{w_{tr}}{a_1}\Big], \tag{20}$$

where XT''_μ and XT'_μ are the mean XT in TA-MCFs and normal step-index MCFs, respectively.

If the mean XT is expressed in dB, we have

$$XT''_{dB} - XT'_{dB} = 10\log_{10}\left\{\Gamma\exp\Big[-4(W_2 - W_1)\frac{w_{tr}}{a_1}\Big]\right\} \approx 10\log_{10}\Gamma - 17.4(W_2 - W_1)\frac{w_{tr}}{a_1}, \tag{21}$$

where 17.4 comes from $40\log_{10} e$.

From Eqs. (9) ~ (13) in [14], we have

$$V_1 = \frac{2\pi}{\lambda} a_1 n_1 \sqrt{2\Delta_1}, \qquad V_2 = \frac{2\pi}{\lambda} a_1 n_0 \sqrt{2|\Delta_2|}, \qquad W_2 = \sqrt{V_2^2 + W_1^2}. \tag{22}$$

Since $n_1 \approx n_0$ and it is assumed that $|\Delta_2|/\Delta_1 = m$, we have $V_2^2 \approx mV_1^2$. For $1.5 \leq V_1 \leq 2.5$ in step-index fibers, an excellent approximation of W_1 can be derived by assuming W_1 is a linear

#217749 - $15.00 USD Received 24 Jul 2014; revised 28 Aug 2014; accepted 8 Sep 2014; published 15 Sep 2014

function of V_1. It can be written as $W_1 = 1.1428V_1 - 0.996$, which is within 0.2% of accuracy over the range of V_1 [16]. Thus

$$W_2 \approx \sqrt{mV_1^2 + W_1^2} = \sqrt{mV_1^2 + (1.1428V_1 - 0.996)^2}. \tag{23}$$

For $1.5 \le V_1 \le 2.5$, W_2 can also be approximated to a linear function of V_1, as listed in Table 1, where $m = 0$ means that there is no trench, which corresponds to normal step-index structure. The approximation accuracies at $m = 1$ and $m = 2$ are within ±0.3%.

Table 1. Approximations of W_2 at Different Values of m

$m = \lvert\Delta_2\rvert/\Delta_1$	W_2		$W_2 - W_1$
0	$1.1428V_1 - 0.996$		0
1	$1.452V_1 - 0.520$		$0.309V_1 + 0.476$
2	$1.750V_1 - 0.388$		$0.607V_1 + 0.608$

4. Results and discussions

4.1. Comparison with numerical simulations

In the previous derivation of the mode coupling coefficient in TA-MCFs, the modified Bessel functions of the 1st kind $I_0(W_1 r/a_1)$ in the 1st cladding and the trench have been ignored. Therefore, the XT obtained using Eq. (5) and the most rigorous finite element method (FEM) could be different. Furthermore, since the simplified analytical expression Eq. (18) is an approximation of the non integrable expression Eq. (5), comparison of the XT based on these two expressions is also needed. The comparison is done based on the structural parameters listed in Table 2, in which the distance from the outer edge of the 1st cladding to the core center a_2 has been assumed to be twice the core radius a_1. The effective area of each core will be reduced if the trench is placed too close to the core, while the trench should be placed as close as possible to the core to reduce core pitch for high core density MCFs. Taking these considerations into account, the ratio of $a_2/a_1 = 2$ seems to be a reasonable choice.

Table 2. Structural Parameters for XT Calculation and Numerical Simulations

Parameters	Trench-assisted	Step-index	Units
a_1	4.5	4.5	μm
a_2/a_1	2	-	-
a_3/a_1	3	-	-
$R_{\mathrm{tr}} = w_{\mathrm{tr}}/a_1$	1	-	-
n_0	1.45	1.45	-
Δ_1	0.35	0.35	%
Δ_2	$-0.35, -0.70$	-	%
R_{b}	140	140	mm
L	100	100	km

where R_{tr} is the ratio of trench width to core radius.

#217749 - $15.00 USD Received 24 Jul 2014; revised 28 Aug 2014; accepted 8 Sep 2014; published 15 Sep 2014

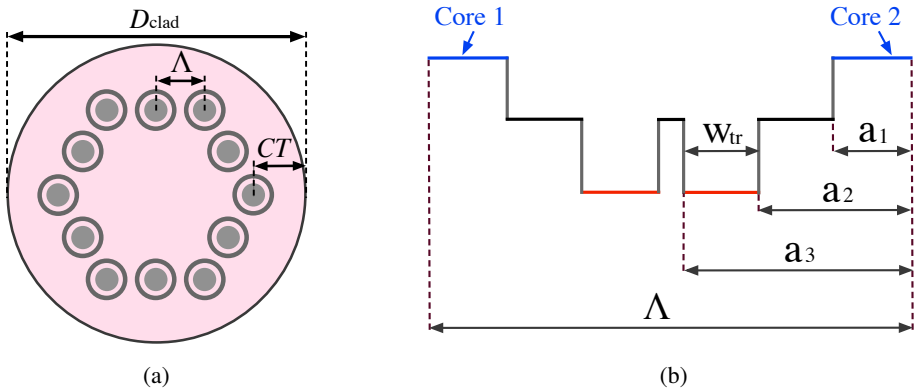

Fig. 2. (a) Cross-sectional view of one-ring structured trench-assisted 12-core MCF and (b) refractive index profiles between adjacent cores with a sufficient large core pitch.

The trench width w_{tr} is now only limited by the core pitch and the distance between adjacent trenches since the trench should not overlap with the neighboring trenches, as shown in Fig. 2. The maximum cladding diameter (D_{clad}) is limited by mechanical reliability [17] since fibers with larger cladding diameters will experience larger tension due to bending. To satisfy the limit of failure probability, the cladding diameter should be less than 225 μm [9]. The cladding thickness (CT) is the distance between the cladding edge and the center of the outermost cores, which is assumed to be at least 30 μm due to micro-bending loss consideration [8]. With these constraints and if the minimum distance between adjacent trenches is assumed to be 3 μm, the core pitch of the one-ring arranged 12-core MCF as shown in Fig. 2(a), should be less than 39 μm. Thus, the maximum distance from the outer edge of trench to the core center would be $a_3 = (39-3)/2 = 18$ μm. With the other parameters listed in Table 2, the allowed trench width w_{tr} has to be less than $2a_1$ (or 9 μm), where $w_{tr} = 4.5$ μm is used in the table. The comparison of XT between analytical calculation and numerical simulations (both for non integrable expression and FEM) for TA-MCFs is plotted in Fig. 3. It should be noted that the XT presented here is only between two adjacent cores for simplicity without assuming any specific core arrangement in MCFs. The length and bending radius of the fiber are assumed to 100 km and 140 mm, respectively. The XT for normal step-index structure is also included for comparison, which can be regarded as trench-assisted structure with $\Delta_2 = 0\%$.

In order to guarantee that the simplified analytical expression has good accuracy for Δ_2 over a wide range, the XT at Δ_2 of both -0.35% and -0.70% are included, where the relative refractive index difference between trench and cladding of $\Delta_2 = -0.70\%$ might be the limit for regular VAD and OVD processes. The trench width should be large enough to reduce the XT and if the minimum trench width is set to be the same as a_1 as in Table 2, the corresponding core pitch would be $2a_3 + 3 = 2 \times 3a_1 + 3 = 30$ μm, in which 3 μm is the minimum distance between adjacent trenches. The numerical simulations based on the non integrable expression Eq. (5) and on FEM are carried out at core pitches of 30, 35, 40 and 45 μm, while the XT calculation using analytical expression Eq. (18) can be plotted over the entire continuous range.

As can be seen from Fig. 3, the XT estimations based on the analytical expression and on the non integrable expression are in good agreement as they almost overlap with each other. In other words, the approximation used to simplify the non integrable expression has very good accuracy. The XT simulated by FEM is always a little lower than the one obtained by the non integrable expression and the analytical expression. For the case at Δ_2 of -0.35%, the maximum

#217749 - $15.00 USD Received 24 Jul 2014; revised 28 Aug 2014; accepted 8 Sep 2014; published 15 Sep 2014

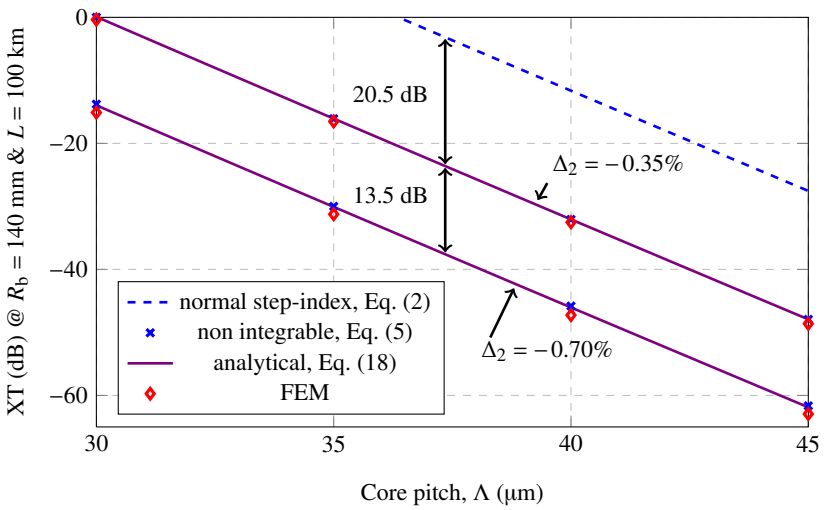

Fig. 3. Crosstalk comparison among analytical calculation and numerical simulations (non integrable expression and FEM) in a trench-assisted MCF as a function of core pitch Λ at 1550 nm, where the trench width equals the core radius. The XT in a normal step-index MCF is included for comparison.

XT difference between analytical expression and FEM is less than 0.7 dB, while for the case when Δ_2 is changed to -0.70%, this difference is increased a little, but is still less than 1.5 dB. Thus the analytical expression can be used to estimate XT with good accuracy without the burden of numerical simulations based on FEM. As can be seen from Fig. 3, the XT curves versus core pitch at different Δ_2 based on the analytical expression seem to be parallel to each other. Referring to Eq. (24), it is also found that the amount of XT reduction in trench-assisted structure relative to normal step-index structure is core pitch independent.

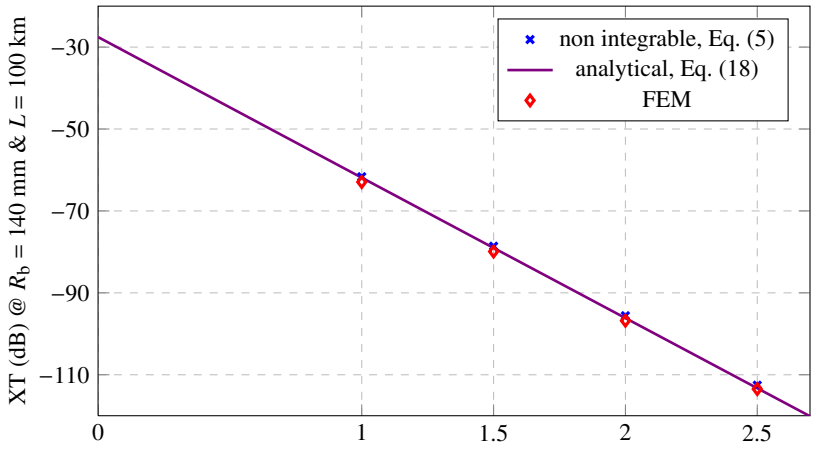

Fig. 4. Crosstalk comparison among analytical calculation and numerical simulations (non integrable expression and FEM) in trench-assisted structure as a function of ratio of trench width to core radius $R_{tr} = w_{tr}/a_1$, at 1550 nm, with core pitch Λ of 45 μm and $\Delta_2 = -0.70\%$.

#217749 - $15.00 USD Received 24 Jul 2014; revised 28 Aug 2014; accepted 8 Sep 2014; published 15 Sep 2014

As discussed previously, the maximum trench width can be larger than core radius depending on the allowed core pitch in high core density MCFs. The XT comparison is then extended to the case when w_{tr} is larger than core radius a_1, as shown in Fig. 4, in which the relative refractive index difference Δ_2 between trench and cladding is set to -0.70%. The numerical simulations based on the non integrable expression and FEM were performed at $R_{tr} = w_{tr}/a_1$ =1.0, 1.5, 2.0 and 2.5, while the XT estimation based on the analytical expression is plotted as a function of the ratio of trench width to core radius, where the XT at $R_{tr} = 0$ corresponds to the normal step-index structure. The core pitch in this comparison is set to be 45 μm for all different ratios of trench width to core radius, thus the distance between adjacent trenches is different for different values of R_{tr}. With the maximum R_{tr} of 2.5, the distance between adjacent trenches is calculated to be 4.5 μm ($= 45 - 2 \times (2 + 2.5) a_1$), which still satisfies the minimum distance requirement between adjacent trenches of 3 μm.

Again, the XT estimations based on the analytical expression agree very well with those obtained by the non integrable expression and FEM at different ratio R_{tr} of trench width to core radius. The XT based on FEM is still a little lower than the one calculated by analytical methods, but the maximum difference is below 1.5 dB for R_{tr} ranges from 1.0 to 2.5, as plotted in Fig. 4. The maximum R_{tr} used in the comparison is 2.5, which is realistic in practical applications. As the trench width is mostly limited by core pitch, and the core pitch in high core density MCFs is normally below 45 μm. It is important to note that the cable cutoff wavelength becomes longer when the trench width increases. For instance, with Δ_2 of -0.70%, the maximum trench width based on numerical simulations is $1.56a_1$ so that the single mode operation is still guaranteed in C band (with corresponding cable cutoff wavelength of 1530 nm). By comparing with the FEM results, it is confirmed that the simplified analytical expression is valid for parameters such as Δ_2 ranging from 0 to -0.70% and trench width from 0 to as large as $2.5a_1$. It should be noted that the distance from the outer edge of the 1st cladding to the core center is always set to twice the core radius in the above XT comparison.

Another issue for MCF transmission is the wavelength-dependent XT, which increases with wavelength. Since the transmission distance in MCFs is determined by the worst XT over the transmission band, it is important to understand the properties of wavelength-dependent XT for high capacity and long distance MCF transmission. TA-MCFs are widely adopted in capacity record transmissions [4, 5] because of their low XT, a theoretical study of the wavelength-dependent XT in TA-MCFs has already been carried out with our simplified analytical expression derived in this work, [12].

4.2. Prospect for further reduction of XT

The mean XT in trench-assisted structure, XT''_{dB} can be obtained by simply adding the term $10\log_{10}\Gamma - 17.4(W_2 - W_1)w_{tr}/a_1$ to the XT in normal step-index structure XT'_{dB} as shown below

$$XT''_{dB} = XT'_{dB} + 10\log_{10}\Gamma - 17.4(W_2 - W_1)\frac{w_{tr}}{a_1}. \tag{24}$$

Based on the above equation, it is easy to find that the XT in TA-MCFs can be reduced by increasing either $W_2 - W_1$ or $R_{tr} = w_{tr}/a_1$. As derived previously, a larger ratio of relative refractive index difference $m = |\Delta_2|/\Delta_1$ results in a larger $W_2 - W_1$. As Δ_1 in trench-assisted structure is set to be the same as in normal step-index structure for easy comparison, the XT reduction can be achieved by increasing the absolute value of the relative refractive index difference $|\Delta_2|$ between trench and cladding. For instance, based on the parameters in Table 2, an increase of $|\Delta_2|$ from 0 to Δ_1 induces a XT reduction of 20.5 dB and an increase of $|\Delta_2|$ from Δ_1 to $2\Delta_1$ introduces a further XT reduction of 13.5 dB, as depicted in Fig. 3.

The relative refractive index difference between trench and cladding Δ_2 is limited to be around -0.70% by regular VAD and OVD processes. Other techniques of further reducing

#217749 - $15.00 USD Received 24 Jul 2014; revised 28 Aug 2014; accepted 8 Sep 2014; published 15 Sep 2014

Δ_2 have been proposed, such as hole-assisted structure [6]. As shown in Fig. 5, if Δ_2 is reduced from -0.70% to -1.40%, a further XT reduction of around 21 dB is possible. It should be noted that an increase of $|\Delta_2|$ or R_{tr} may result in a longer cable cutoff wavelength, since the mode will be strongly confined in TA-MCFs. For instance, in order to have single mode operation in C band, the maximum trench width is only $0.96a_1$ at Δ_2 of -1.40%, based on numerical simulations.

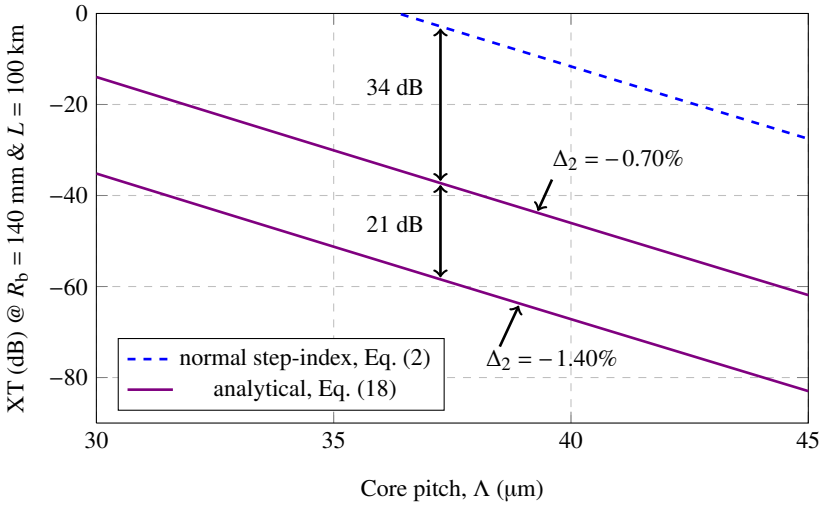

Fig. 5. Further reduction of XT by changing Δ_2 from -0.70% to -1.40%, based on analytical expression in trench-assisted structure versus core pitch Λ, at 1550 nm with trench width equal to core radius.

If the ratio of refractive index difference m and the ratio of trench width to core radius R_{tr} are fixed, XT in TA-MCFs can be reduced by increasing V_1, as can be seen from Table 1. Since V_1 is the V number at the transmission wavelength, in order to have a higher V_1, the theoretical cutoff wavelength (at which, $V_1 = 2.405$) should be shifted from the shorter wavelength towards the lower end of C band (1530 nm). In real applications, cable cutoff wavelength is more practically used, and it might be longer than theoretical cutoff wavelength, depending on trench volume ($|\Delta_2|$ and w_{tr}) and core pitch. If cable cutoff wavelength (which must be shorter than 1530 nm to guarantee single mode operation if both C + L bands are used for high capacity transmission) is longer than theoretical cutoff wavelength, then V_1 will be smaller, which means the mode is less confined, resulting in worse XT.

5. Conclusion

An analytical expression for the mode coupling coefficient in homogeneous TA-MCFs is derived, which has a very simple relationship with the one in homogeneous normal step-index MCFs. With this analytical expression, the XT in MCFs with a trench-assisted structure can easily be calculated and plotted directly without the need of numerical simulations. Comparison with the most exact FEM simulations confirms that this analytical expression has very good accuracy, thus is very useful as a powerful design tool. This analytical expression can be used to quickly estimate the XT in trench-assisted MCFs and analyze the relationships between XT and various fiber parameters. Based on these analytical relationships and if the core pitch is fixed, it is found that the XT between adjacent cores in TA-MCFs is ultimately limited by the relative refractive index difference between trench and cladding, and the trench width due to

#217749 - $15.00 USD Received 24 Jul 2014; revised 28 Aug 2014; accepted 8 Sep 2014; published 15 Sep 2014

core pitch limitation for high core density. The XT properties, such as XT dependence on core pitch and wavelength-dependent XT can be analyzed based on the analytical expression.

Acknowledgments

The authors would like to thank Dr. Yutaka Miyamoto and Dr. Hidehiko Takara of NTT Network Innovation Labs., Dr. Shoichiro Matuso and Dr. Katsuhiro Takenaga of Fujikura Ltd. for furuitful disucussions.

#217749 - $15.00 USD Received 24 Jul 2014; revised 28 Aug 2014; accepted 8 Sep 2014; published 15 Sep 2014